DARWINIANA
NUEVA SERIE
www.ojs.darwin.edu.ar
ISSN 0011-6793 impresa - ISSN 1850-1699 en línea

DARWINIANA, nueva serie 13(1): 74-89. 2025
Versión de registro, efectivamente publicada el 25 de marzo de 2025
DOI: 10.14522/darwiniana.2025.131.1273

RED TIDE-FORMING DINOFLAGELLATES FROM ARGENTINEAN COASTAL WATERS: INSIGHTS INTO *GYMNODINIUM CATENATUM* (DINOPHYCEAE) AND FIRST RECORD OF *G. IMPUDICUM*

Delfina Aguiar Juárez[1,2,*], Jorge I. Mardones[3,4], Luis Norambuena[3], Javier Paredes-Mella[3], Eugenia A. Sar[1,2], Ana Flores-Leñero[5], & Inés Sunesen[1,2,**]

[1] *División Ficología Dr. Sebastián Guarrera, Facultad de Ciencias Naturales y Museo (FCNyM), Universidad Nacional de La Plata, Paseo del Bosque s/n, 1900, La Plata, Argentina; *delfina.aguiar@fcnym.unlp.edu.ar **isunesen@fcnym.unlp.edu.ar* (authors for correspondence).
[2] *Consejo Nacional de Investigaciones Científicas y Técnicas (CONICET), Godoy Cruz 2290, C1425FQB, Ciudad Autónoma de Buenos Aires, Argentina*.
[3] *Centro de Estudios de Algas Nocivas (CREAN), Instituto de Fomento Pesquero (IFOP), Padre Harter 574, 5480000, Puerto Montt, Chile*.
[4] *Centro de Investigaciones en Recursos Naturales y Sustentabilidad (CIRENYS), Universidad Bernardo O'Higgins, Viel 1497, 8370993, Santiago, Chile*.
[5] *Scottish Association for Marine Science, Scottish Marine Institute, Oban, Argyll, PA371QA, Scotland, UK.*

Abstract. Aguiar Juárez, D.; J. I. Mardones, L. Norambuena, J. Paredes-Mella, E. A. Sar, A. Flores-Leñero & I. Sunesen. 2025. Red tide-forming dinoflagellates from Argentinean coastal waters: insights into *Gymnodinium catenatum* (Dinophyceae) and first record of *G. impudicum*. *Darwiniana*, nueva serie 13(1): 74-89.

As a part of a monitoring program of harmful microalgae in the coastal waters of Buenos Aires Province, two strains of chain-forming *Gymnodinium* species (Dinophyceae), LPCc043 and LPCc044, were isolated from samples collected in Samborombón Bay. This study aims to provide a morphological, phylogenetic and toxicological characterization of the strains. Among marine chain-forming *Gymnodinium* species, only *G. catenatum* and *G. impudicum* are known to form harmful algal blooms (HAB). Morphological analysis with light and electron scanning microscopy (LM, SEM) revealed that strain LPCc043 had larger cells, a higher number of cells per chain, and an acrobase independent of the sulcus entering the epicone, whereas strain LPCc044 had smaller cells, a lower number of cells per chain, and an acrobase as an extension of the sulcus. Phylogenetic analysis based on partial LSU rDNA sequencing placed the sequence corresponding to strain LPCc043 in the *G. catenatum* clade and that corresponding to strain LPCc044 in the *G. impudicum* clade with a 99–1.0 and 100–1.0 bootstrap and Bayesian posterior probability, respectively. Toxicological analysis by hydrophilic interaction liquid chromatography with tandem mass spectrometry (HILIC-UHPLC-MS/MS) detected paralytic shellfish toxins (PSTs) in *G. catenatum*, predominantly N-sulfocarbamoyl-11-hydrosulfate toxin 1/2 (C1/C2) and decarbamoyl gonyautoxin 2/3 (dcGTX2/3). In contrast, no PST were found in *G. impudicum*. This study contributes to the knowledge of harmful algal species diversity along the Argentinean coast and highlights the importance of monitoring these species for public health and environmental management.

Keywords. Atlantic Ocean; Harmful Algal Blooms (HAB); Paralytic Shellfish Toxins (PST); Phylogeny; Toxicology.

Resumen. Aguiar Juárez, D.; J. I. Mardones, L. Norambuena, J. Paredes-Mella, E. A. Sar, A. Flores-Leñero & I. Sunesen. 2025. Dinoflagelados formadores de mareas rojas en aguas costeras argentinas: perspectivas sobre *Gymnodinium catenatum* (Dinophyceae) y primer registro de *G. impudicum*. *Darwiniana*, nueva serie 13(1): 74-89.

Como parte de un programa de monitoreo de microalgas nocivas en las aguas costeras de la Provincia de Buenos Aires, se aislaron dos cepas formadoras de cadenas del género *Gymnodinium*

Original recibido el 24 de enero de 2025, aceptado el 12 de marzo de 2025
Editor Asociado: Fernando Biganzoli

(Dinophyceae), LPCc043 y LPCc044, a partir de muestras colectadas en la Bahía Samborombón. Este estudio tiene como objetivo proporcionar una caracterización morfológica, filogenética y toxicológica de las cepas aisladas. Entre las especies marinas de *Gymnodinium* formadoras de cadenas, solo *G. catenatum* y *G. impudicum* son conocidas como productoras de florecimientos algales nocivos (FAN). El análisis morfológico mediante microscopía óptica y electrónica de barrido (MO, MEB) reveló que la cepa LPCc043 tenía células más grandes, un mayor número de células por colonia y una acrobase independiente del sulcus que penetra en el epicono, mientras que la cepa LPCc044 presentaba células más pequeñas, un menor número de células por colonia y una acrobase como una extensión del sulcus. El análisis filogenético basado en la secuenciación parcial del ADN ribosomal LSU colocó a la secuencia correspondiente a la cepa LPCc043 en el clado de *G. catenatum* y a la correspondiente a la cepa LPCc044 en el de *G. impudicum*, con valores de bootstrap y probabilidad posterior bayesiana de 99–1.0 y 100–1.0, respectivamente. El análisis toxicológico mediante cromatografía líquida de interacción hidrofílica con espectrometría de masas en tándem (HILIC-UHPLC-MS/MS) detectó toxinas paralizantes de moluscos (TPM) en *G. catenatum*, predominantemente N-sulfocarbamoil-11-hidrosulfato toxina 1/2 (C1/C2) y decarbamoil goniautoxina 2/3 (dcGTX2/3). En contraste, no se detectaron TPM en *G. impudicum*. Este estudio contribuye al conocimiento de la diversidad de especies de algas nocivas a lo largo de la costa argentina y destaca la importancia de monitorear estas especies para la salud pública y la gestión ambiental.

Palabras clave. Filogenia; Floraciones Algales Nocivas (FAN); Océano Atlántico; Toxicología; Toxinas Paralizantes de Moluscos.

INTRODUCTION

Gymnodinium catenatum Graham (Dinophyceae, Gymnodiniales) is the only unarmoured dinoflagellate known to produce paralytic shellfish toxins (PST) (Anderson et al., 1989; Oshima et al., 1993; Rees & Hallegraeff, 1991; Taylor et al., 2004). This chain-forming species was first described from the Gulf of California (Graham, 1943) and later identified in Argentinean coastal waters during summer-autumn 1962 (Balech, 1964), although its potential ability to produce toxins was unknown at the time. It is widely distributed worldwide and has been linked to Harmful Algal Blooms (HAB) and paralytic shellfish poisoning (PSP) outbreaks across different parts of the world (Bustillos-Guzmán et al., 2015; Lassus et al., 2016 and references therein).

The first evidence linking *G. catenatum* to PSP outbreaks came from the Galician Rias, Spain, and the Gulf of California, Mexico. In these regions, the ingestion of bivalves associated with the presence of this species in the water column led to severe PSP events (Estrada et al., 1984, from the Galician rias, Spain; Mee et al., 1986, from Mazatlán, Gulf of California, México), some of which resulted in human fatalities and extensive fish kills (Mee et al., 1986). In South America, PSP outbreaks of *G. catenatum* occur mostly in late summer or early autumn, in Uruguay, Brazil and Argentina (Carreto & Akselman, 1996; Proença et al., 2003; Medina et al., 2003). In Uruguay, the first toxic episode associated with this species in the Southwestern Atlantic Ocean was reported in 1992 (Méndez & Ferrari, 2003), leading to the detection of PSTs in shellfish and resulting in harvesting bans to protect human health (Méndez & Ferrari, 2003; Méndez & Carreto, 2018). Similarly, in Argentina, *G. catenatum* has been linked to HAB in Buenos Aires Province (Akselman et al., 1998; Montoya et al., 2006; Sunesen et al., 2014), with its toxin profile characterized from field samples collected in Mar del Plata during a bloom in 2003 (Montoya et al., 2006). During the years 2008 and 2009, positive bioassays for PSTs were obtained, associated with the presence of *G. catenatum* at concentrations of 10^3 to 10^4 l^{-1}, leading to a ban on shellfish consumption and extraction (Sunesen et al., 2014).

The toxin profile of *G. catenatum* was first characterized using culture material from inshore Tasmanian waters, Australia (Oshima et al., 1987). Currently, this species is known to produce saxitoxin (STX), decarbamoyl saxitoxin (dcSTX), N-sulfocarbamoyl gonyautoxins (GTX1-GTX4), and the less toxic N-sulfocarbamoyl-11-hydroxysulfate B- and C-toxins (Bl, B2 and Cl-C4), deoxy-decarbamoyl saxitoxin (doSTX), deoxy-decarbamoyl gonyautoxin 3 (doGTX3), and benzoyl saxitoxin analogs (GC toxins), with profiles varying by geographical origin of the studied strains and culture conditions (Band-Schmidt et al., 2020; Liu et al., 2020, and references therein).

Another chain-forming species of *Gymnodinium*, *G. impudicum* (Fraga & Bravo) G.Hansen & Moestrup (Daugbjerg et al., 2000), has been described as a non-toxic species HAB producer (Fraga et al., 1995), mainly distributed in temperate areas (Fraga et al., 1995; Luo et al., 2018). Despite the morphological similarities

between *G. catenatum* and *G. impudicum* (Fraga et al., 1995), phylogenetic analysis based on partial LSU rDNA sequences revealed that *G. impudicum* is more closely related to species of *Barrufeta* N.Sampedro & S.Fraga than to *G. catenatum* (Luo et al., 2018).

In the framework of a phytoplankton and biotoxin monitoring program implemented in Samborombón Bay (Buenos Aires Province, Argentina), an important breeding area for fish, two chain-forming *Gymnodinium* strains (LPCc043 long chains and LPCc044 short chains) were isolated.

This study aims to provide an identification and characterization of chain-forming HAB species of the genus *Gymnodinium* based on morphology, phylogeny (using LSU rDNA sequencing) and toxicology, and to compare these results with those found in the literature, enhancing the knowledge of their diversity and ecological significance in Argentinean coastal waters.

MATERIALS AND METHODS

Study area

The Río de la Plata, located between 34° 00' - 36° 20' S and 55° - 58° W, spans an area of 35,500 km^2, draining the second largest basin in South America. This extensive, shallow, coastal plain estuary discharges into the Southwestern Atlantic Ocean with a total flow of 20,000–25,000 m^3 s^{-1} (Framiñan & Brown, 1996). Due to its large size and environmental diversity, it is divided into freshwater and mixohaline regions (Gómez et al., 2004), separated by the submerged Barra del Indio barrier, which extends from Punta Piedras (Argentina) to Montevideo (Uruguay) (Acha et al., 2008). In this area, a salinity front controlled by topography that gives rise to a well-developed turbidity front, which aligns with the Samborombón Bay geometry (Framiñan & Brown, 1996).

The mixohaline region has a quasi-permanent salt wedge regime, with tidal velocities typically below 45 cm s^{-1}, resulting in a two-layer system with a strong vertical stratification. Its large extension and shallow depth also make it highly susceptible to atmospheric forcing (Acha et al., 2008).

Isolation and culture of microalgae strains

Cells of *Gymnodinium* were collected in February 2021 from Tapera de López (36° 19.30' S - 56° 46.43' W, Samborombón Bay, Fig. 1) using a 30 µm mesh phytoplankton net. Sampling was conducted as a part of a monitoring program for harmful phytoplankton and shellfish toxins. Strains isolation was carried out using a micropipette under a Zeiss Axiovert 40 CFL inverted microscope. Two isolates, LPCc043 (long chain-forming) and LPCc044 (short chain-forming), were kept in filtered estuarine water enriched with f/2 medium (Guillard, Sigma Aldrich, Saint Louis, MO, USA) and incubated at 16 °C and 12:12 h light:dark cycle following Sunesen et al. (2020).

Microscopy

Light microscopy (LM). Live cells were observed using a Zeiss Axiovert 40 CFL inverted microscope equipped with phase contrast and differential interference contrast (DIC) and an AxioCam 208c digital camera (Zeiss Microimaging, Goettingen, Germany), and a Leica DMLA microscope equipped with DIC and a Leica DFC420c digital camera (Leica Microsystems, Wetzlar, Germany). Cell counts of samples were carried out using a Zeiss Axiovert 40 CFL inverted microscope with the Utermöhl technique (Utermöhl, 1958).

Scanning Electron Microscopy (SEM). Cultured material was processed following the procedure described by Fraga et al. (1995) with minor modifications. Aliquots of 6 ml of cultures were collected and transferred into 15 ml Falcon tubes, which were left to stand at room temperature for 30 min. The material was then fixed with 2.5% glutaraldehyde. Following fixation, the samples were filtered through Isopore filters (3 µm pore size, TSTPO1300) and filters were placed in filter paper envelopes. These envelopes were transferred to a beaker and washed 3 times with culture medium for 15 min each. Subsequently, the samples were post-fixed with 1% osmium tetroxide (OsO4) in culture medium for 1 h at 4 °C. After post-fixation, the fixative was removed by washing the samples three times with distilled water for 15 min each. The samples were then dehydrated at 4 °C with an increasing battery of ethanol at 10%, 20%, 30%, 40%, 50%, 60%, 70%, 80%, 96% for 15 min at each concentration, and twice at 100%. After dehydration, critical point drying was performed in an HCP-2 (Hitachi). The filters were mounted on 12.7 mm diameter slides previously covered with carbon adhesive tape. Finally, the samples were metallized with gold–palladium.

DNA extraction, amplification, sequencing and phylogeny

Genomic DNA was obtained harvesting strains LPCc043 and LPCc044 in exponential phase of growth with the Plan Genomic DNA Purification Kit (Thermo Fisher Scientific, USA), following the Manufacturer's protocol. The LSU (D1-D2) rDNA region was amplified using primers D1R and D2C (Scholin et al., 1994; Edvardsen et al., 2003). PCR included an initial denaturation step of 95 °C for 5 min, followed by 40 cycles of 95 °C for 1 min, 55 °C for 1:20 min, 72 °C for 2 min, followed by

a 10 min extension at 72 °C. The PCR products of both genes were visualized on a 1.5% agarose gel and sent to Macrogen Sequencing Facility (Macrogen®, Seoul, South Korea). Phylogenetic analyses were performed using alignments of 678 bp with sequences available in GenBank using ClustalX multiple alignment (Larkin et al., 2007). A list of species included in the phylogenetic reconstructions is given in Table S1.

Phylogenetic reconstruction was inferred using maximum likelihood (ML) method involving Tamura-Nei model (Tamura & Nei, 1993) as the best evolutionary model for ML. Node reliability was estimated through bootstrap analysis (1,000 replicates). Net mean *p*-distances between strains LPCc043 and LPCc044 and other clades were calculated. No corrections for multiple substitutions at the same site, substitution rate biases (e.g. differences in the transitional and transversional rates), or differences in evolutionary rates among sites were considered (Nei & Kumar, 2000). These analyses were performed using MEGA X software (Kumar et al., 2018).

Additionally, a Bayesian inference (BI) analysis was conducted by sampling across the entire GTR model space using MrBayes V3.2 (Huelsenbeck & Ronquist, 2001). Finally, a sequence from *Noctiluca scintillans* (Macartney) Kofoid and Swezy was used to root the LSU rDNA tree.

Toxin extraction and analysis

Aliquots of 5 ml of cultures of strains LPCc043 and LPCc044 were collected to assess cell density by LM using a Sedgewick-Rafter chamber. Cultures were harvested during the mid-exponential growth phase for toxin analysis. Culture samples of 15 ml were filtered through 25 mm diameter glass fiber filters (Whatman GF/C, 1.2 mm nominal pore size) and transferred to 2 ml plastic tubes. To each tube, 0.5 ml of acetic acid (0.05 M) and approximately 0.9 g of Lysing Matrix D (MP Biomedicals, USA) were added. Tubes were homogenized using a minibead beater-16 cell disruptor (BioSpect Products, USA) for 45 s and centrifuged in a mini-spin centrifuge (Eppendorf, Germany) at 12,100 *g* during 5 min. The supernatant was filtered through a 0.22 µm pore size 3 mm diameter PVDF syringe filter. Aliquots of 200 µl were diluted with 600 µl of acetonitrile, transferred into HPLC vials, which were then stored at -20 °C until further analysis.

Chromatographic separation was performed using a 1290 Infinity II ultra-high performance

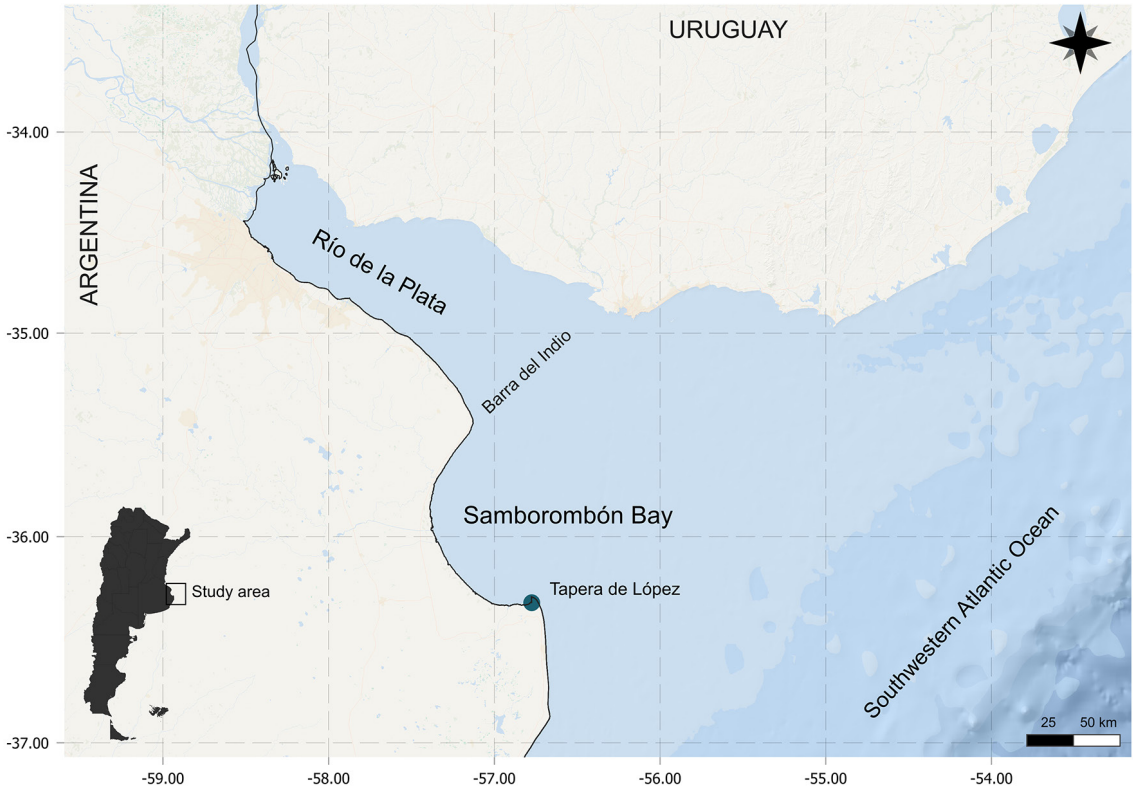

Fig. 1. Study area showing the sampling site location.

liquid chromatography system (UHPLC) coupled to an Agilent 6420A Triple Quadrupole mass spectrometer with an electrospray ionization (ESI) source (Agilent, Palo Alto, CA, USA), following the method described by Rodríguez et al. (2018). Separation of paralyzing toxins by HILIC was carried out using an Acquity UHPLC BEH Amide column (100 × 2.1 mm, 1.7 µm, Waters) at 35 °C, with an injection volume of 5 µl. Mobile phase A was 100% water with 0.1% formic acid and 10 mM ammonium formate. Mobile phase B was MeCN containing 0.1% formic acid and 2% 100 mM ammonium formate solved in water. The separation was performed using a gradient elution method at a flow rate of 0.4 ml/min, starting with 90% mobile phase B, followed by a linear gradient to 21% B over 7 min. The gradient returned to the initial conditions in 0.1 min, with a total run time of 13.5 min.

Mass spectrometric parameters were as follows: capillary voltage: 3.5 kV in positive ion mode and 3.0 kV in the negative ion mode, gas flow at 10 l min^{-1}, gas temperature at 300 °C, and nebulizer pressure at 30 psi. The collision energy and cell accelerator voltages were optimized for each analog, as detailed in Table S2. Mass spectrometric analyses for GC analogs were carried out using the of GC-transitions described by Durán-Riveroll et al. (2017).

Certified standard solutions for PST (C1 and C2, GTX1 and GTX4, GTX2 and GTX3, B1 (formerly GTX5), B2 (formerly GTX6), dc GTX2 and dcGTX3, dcSTX, STX, dcNEO, NEO) were obtained from the National Research Council of Canada (NRCC, Halifax, Canada).

RESULTS

Environmental data

Both chain-forming strains of *Gymnodinium* (LPCc043 and LPCc044) were found in February 2021, in the same sample (Herbarium code LPC13727), at low abundances (1,000 cells l^{-1}). No bloom was observed during the sampling period. The accompanying phytoplankton community was dominated by diatoms, phytoflagellates < 5 µm and other small dinoflagellates. No chains were found, only isolated cells of *Gymnodinium* were present. The water temperature was 23.6 °C, and the salinity was 20.

Morphological analysis

Gymnodinium catenatum Graham
Fig. 2 A–H.

References: Graham, 1943: 259, figs 1, 2; Rees & Hallegraeff, 1991: 91, figs 1–25; Liu et al., 2020: 6, fig. 2 A–I, fig. 3 A–H.

Cells in long chain shaped colonies, sixteen to sixty-four celled in field samples, and four to two celled or solitaries in cultures. Solitary cells, 45–74 µm long (56.8 ± 1.3) and 33–53 µm wide (41.9 ± 1.0) (n = 40), larger than colonial cells, 29–53 µm long (41.7 ± 1.6) and 30–44 µm wide (37.5 ± 0.9) (n = 28). Cell shape with conical, truncate epicone and flattened hypocone in solitaries and colonial specimens (Fig. 2A–F), hypocone exceeding the epicone. Cingulum descending with displacement between 1/5 and 1/6 of a body length about one cingular width (Fig. 2A–C). Sulcus running from the cingulum to the antapex and penetrating straight to the episome near to the independent horseshoe-shaped acrobase or apical groove (Fig. 2G, I). Cells with chloroplasts greenish-yellow to golden brown, numerous, irregular and elongated in shape. Nucleus ovoid to roundish, large, and situated centrally or at left of the mid-ventral plane (Fig. 2D, E). Amphiesma with a honeycomb-like pattern of surface vesicles completely covering the cell and outlining the acrobase and the margins of the cingulum (Fig. 2G, H).

Gymnodinium impudicum (Fraga & Bravo) G. Hansen & Moestrup
Fig. 3A–E.

References: Fraga et al., 1995: 515, figs 1–16 (as *Gyrodinium impudicum*); Daugbjerg et al., 2000: 305; Luo et al., 2018: 750, fig. 7 A–G, fig. 8 A–F.

Cells in short chain shaped colonies, four celled in field samples and two celled or solitaries in cultures. Solitary cells, 29–42 µm long (34.5 ± 1.2) and 20–30 µm wide (24.9 ± 0.9) (n = 27), larger than colonial cells, 23–33 µm long (27.7 ± 0.5) and 21–28 µm wide (24.2 ± 0.3) (n = 36). Cell shape with conical epicone and flattened hypocone in solitary specimens (Fig. 3B, C) and variable according with the position of the cell in the chain in colonial specimens (Fig. 3D). Cingulum descending with displacement between 1/3 and 1/4 of the body length (Fig. 3A, B, D). Narrow sulcus running from the cingulum to the antapex and penetrating to the episome (Fig. 3D, E). Sulcus encircling the apex and forming the acrobase or apical groove (Fig. 3B, C, E arrowheads). Cells with numerous greenish chloroplasts and spherical pusule located towards the right side of the sulcus (Fig. 3A–C).

Molecular phylogeny

Phylogenetic relationships were inferred using an alignment comprising 54 taxa sequences including 10 *Gymnodinium* species and both studied strains (LPCc043, GenBank accession number OP850345; and LPCc044, GenBank accession number OP851763; Table S1). The maximum likelihood and the Bayesian phylogenetic analyses

placed the LPCc043 strain in the *G. catenatum* clade and the LPCc044 strain in the *G. impudicum* clade, both with strong support (99% and 100%, respectively) and by a probability value of 1.0 (Fig. 4).

Within the clades of *G. catenatum* and *G. impudicum*, the Argentinean sequences showed a genetic distance of 0.001 and 0.003 against the sequences reported from other geographical areas, respectively. The genetic distance between both clades was 0.237.

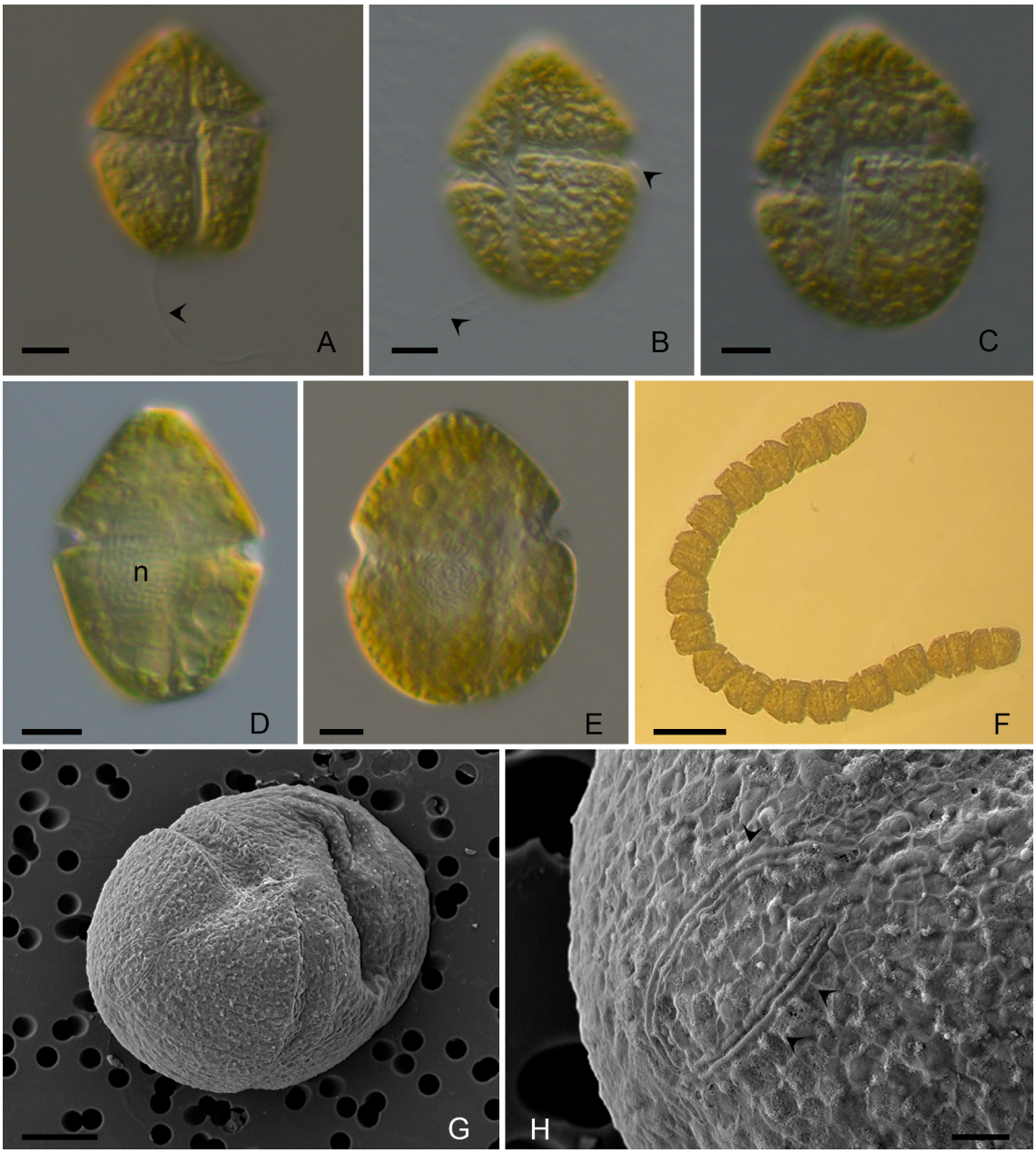

Fig. 2. Cells of *Gymnodinium catenatum* LPCc043 strain during exponential growth phase. **A-D**. Light microscopy. **A-C**. Cells in ventral view. Note the sulcus flagellum (A, arrowhead) and both flagella (**B,** arrowheads). **D-E**. Cells in dorsal view. **F**. Chain of 16 cells. **G-H**. Scanning electron microscopy. **G**. Cell with distorted morphology seen from the apex. **H**. Detail of Fig. G showing the acrobase. Scale bars = 10 µm (A-G), 2 µm (H).

Toxicological analysis

Paralytic shellfish toxins (PST) were found in *Gymnodinium catenatum* strain, but not in *G. impudicum* strain. The toxin profile of *G. catenatum* was predominantly composed of N-sulfocarbamoyl toxin C1/C2, which accounted for 55.8% of the total toxin content, followed by decarbamoil toxins dcGTX2/dcGTX3 at 42.7%, and a minor amount of GTX2/GTX3 (1.5%) (Table 1). No carbamate toxins (STX, GTX1, GTX4), N-sulfocarbamoyl toxins (B1, B2), or decarbamoyl toxins (dcSTX, dcNEO) were detected, with a limit of detection of < 0.01 µM. The calculated cellular toxin content of *G. catenatum* was 17.83 fmol per cell, and the

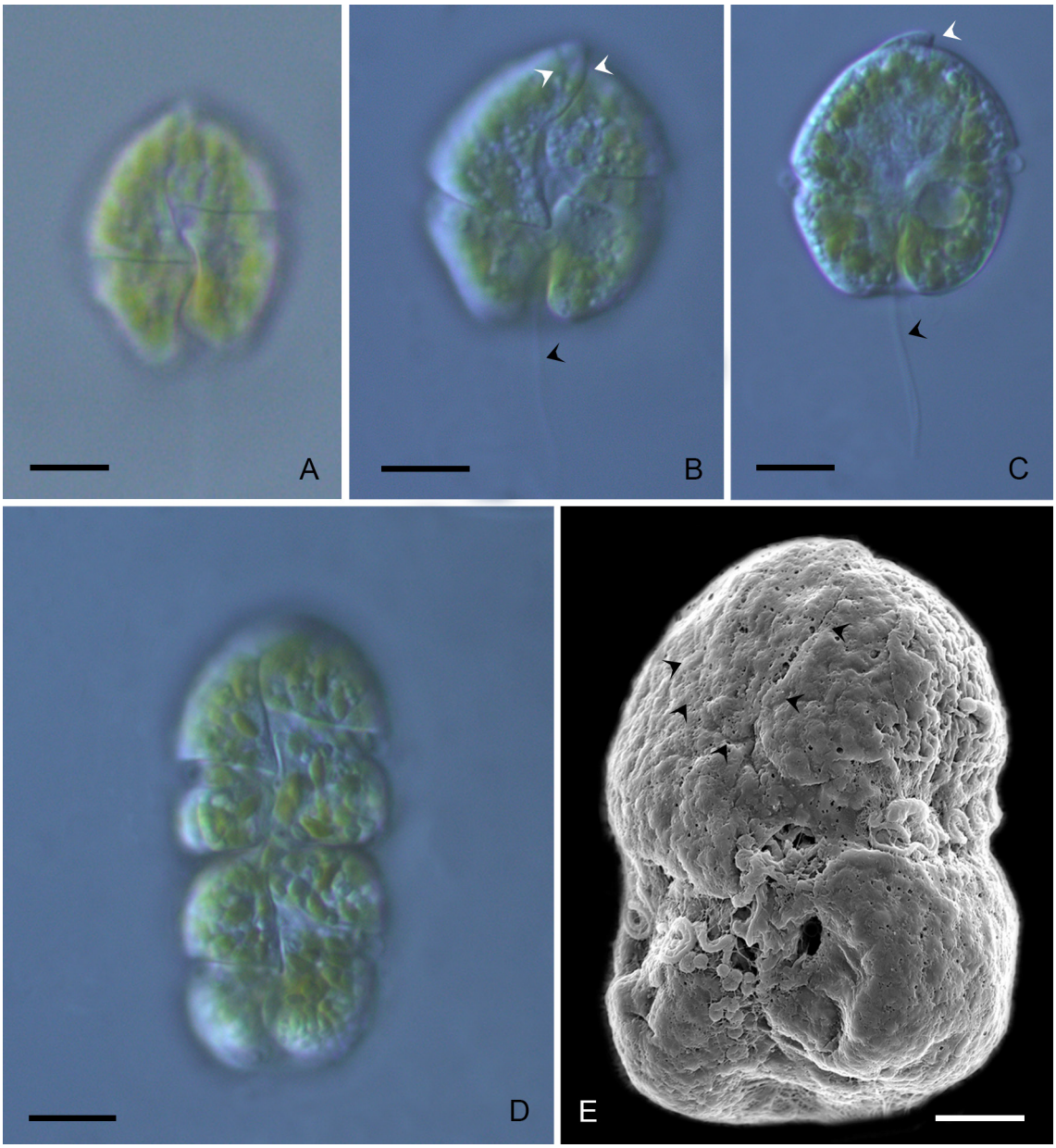

Fig. 3. Strain LPCc044 of *Gymnodinium impudicum* during exponential growth phase. **A-D**. Light microscopy. **A-B**. Cells in ventral view. Note the sulcus flagellum (**B**, black arrowhead) and acrobase (B, white arrowhead). **D**. Chain of two cells in ventral view. **E**. Scanning electron microscopy. Cell in lateral-ventral view. Note the acrobase formed by the sulcus (arrowheads). Scale bars = 10 µm.

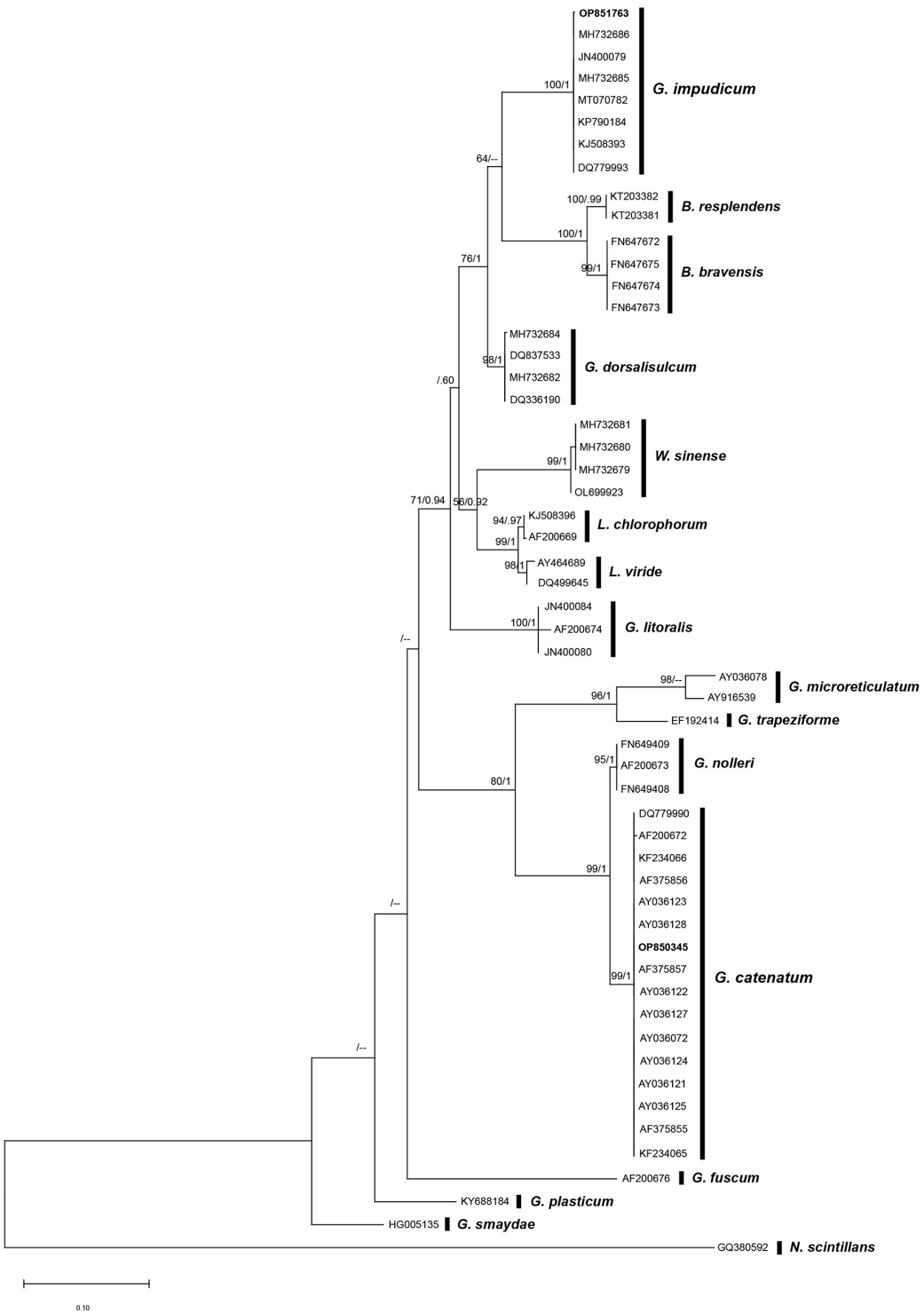

Fig. 4. Maximum likelihood (ML) tree based on the large subunit (LSU rDNA) of Argentinean sequences of *Gymnodinium* and related species. In bold are the sequences analyzed in this study. Branch support is shown as ML/ Bayesian Inference (BI). Only values > 60% (ML) or > 0.6 (BI) are displayed.

Table 1. Toxin profile, toxin content and toxicity of *G. catenatum* strain from Buenos Aires coastal waters. Gonyautoxins (GTXs), N-sulfocarbamoyl toxins (Cs, B1, B2), saxitoxins (STX), NeoSXT (Neo), decarbamoyl toxins (dcGTXs, dcSTX, dcNeo). Nd = not detected.

Toxins	*G. catenatum*		
	%mol	Toxin Content (fmol cell^{-1})	Toxicity (pg STX eq. cell^{-1})
C1/C2	55.8	10	0.5
GTX1/GTX4	Nd	Nd	Nd
GTX2/GTX3	1.5	0.23	0.1
B1	Nd	Nd	Nd
B2	Nd	Nd	Nd
dcGTX2/dcGTX3	42.7	7.6	0.6
dcSTX	Nd	Nd	Nd
dcNeo	Nd	Nd	Nd
SXT	Nd	Nd	Nd
Neo	Nd	Nd	Nd
Total	100	17.83	1.2

corresponding cellular toxicity was 1.20 pg STX equivalents per cell (Table 1).

Additionally, two compounds, suspected to be GC-type toxins, were detected. These compounds exhibited retention times shorter than all the analogues present in the standard solutions used (data not shown), suggesting that they may be more nonpolar compounds in nature. One of these compounds displayed a signal with m/z 473, which fragmented to produce ions at m/z 455, 393 and 375, and was suspected to correspond to GC1 or GC2. However, due to the absence of reference standards solutions for these analogues, their identification could not be conclusively confirmed. The other notable signal corresponded to the transition 393>375, 273, which may correspond to GC6.

DISCUSSION

The marine, chain-forming species *Gymnodinium catenatum* and *G. impudicum* were morphologically characterized and distinguished from each other based on cell size, displacement of the cingulum, number of cells in the chain, and sulcus-acrobase relationship (Fraga et al., 1995; Daugbjerg et al., 2000). *Gymnodinium catenatum* had larger cells, cingulum displaced between a 1/5 and 1/6 of a body length, a greater number of cells in the colony up to 64 and horseshoe-shaped acrobase independent of the sulcus entering the epicone while *G. impudicum* had smaller cells, cingulum displaced between 1/3 and 1/4 of the body length, with a lower number of cells up to 4 in the colony and acrobase formed by the extension of the sulcus encircling the apex. Argentinean strains of both species showed differences in the cell size with most of the previously described (Graham, 1943; Balech, 1964; Fraga et al., 1995; Daugbjerg et al., 2000), being consistently greater in many cases.

Phylogenetic analyses revealed the clustering of the Argentinean strains LPCc043 and LPCc044 within the *G. catenatum* and *G. impudicum* clades, respectively. The low genetic distance of the Argentinean isolates against sequences isolated from the Northern hemisphere, along with the high values of clades reliability (pb and bootstraps), supports the species taxonomic assignments. The phylogenetic topology placed the *G. catenatum* isolate in the same subclade than *G. nolleri* M.Ellegaard & Moestrup with a sister clade grouping *G. trapeziforme* Attaran-Fariman & Bolch and *G. microreticulatum* C.J.S.Bolch & G.M.Hallegraeff. A similar topology was revealed by Attaran-Fariman et al. (2007), Reñé et al. (2011) and Luo et al. (2018). Conversely, phylogenetic topology placed the LPCc044 isolate in same subclade than *Barrufeta bravensis* and *B. respendens* (Hulburt) H.Gu, Z.Luo & K.N.Mertens in concordance with previous studies by Reñé et al. (2011), Gu et al. (2015) and Luo et al. (2018).

The toxin profile of *G. catenatum* isolates

was similar to that determined by Montoya et al. (2006) on a field sample collected at a permanent monitoring station of Mar del Plata, Argentina, except for the presence of GTX4 in the latter, no detected in the former. In both profiles B1, B2 and STX are lacking. The proportions of each toxin on a molar basis are dissimilar, with lesser amounts of toxins C1/C2 and GTX2/GTX3 and greater amounts of dcGTX2/dcGTX3 in our cultured material than in plankton material analyzed by Montoya et al. (2006). A review published by Hallegraeff et al. (2012) shows that there is a great variation both at the intra-population and regional level, regarding the presence of STX derivatives, as well as in their quantity.

The calculated toxin content of 17.83 fmol per cell for the LPCc043 strain was notably lower than the 122 fmol per cell reported by Montoya et al. (2006). However, it falls within the range reported by Negri et al. (2007, Table 2) for strains from different geographical regions with varying toxin profiles. The presence of C3/C4 analogues of paralytic shellfish toxins in the LPCc043 strain is possible, as has been observed in other regions of the world (Hallegraeff et al., 2012). However, their identification could not be confirmed in this study, as these analogues were not included in the analytical method. Due to the unavailability of reference standards for *G. catenatum* (GC) toxins, an attempt was made to detect potential GC toxins by incorporating transitions corresponding to various GC analogues reported by Durán-Riveroll et al. (2017). This approach resulted in the detection of two signals, which are suspected to correspond to one of these toxins, as *G. catenatum* is known to produce these analogues (Hallegraeff et al., 2012). Finally, these results confirmed that *G. impudicum* is a non-toxic species, consistent with the findings of Fraga et al. (1995) based on field samples of the species collected off Valencia and Catalonia coasts during conspicuous blooms, and the lOB strain from Laguna de Fusaro.

This study provides the first record of *G. impudicum* in Argentina and the Southwestern Atlantic Ocean, along with the first morphological, phylogenetic and toxicological characterization of *G. catenatum* and *G. impudicum* based on cultured strains from Argentinean coastal waters. The findings confirm that *G. catenatum* exhibits a distinct toxin profile, while *G. impudicum* was confirmed as a non-toxic species. The potential presence of novel toxin analogues in *G. catenatum* further emphasizes the need for detailed toxin profiling in the region.

These results confirms the co-occurrence of both species in Samborombón Bay, as previously reported in Koran coastal waters, Kuwait Bay in the Arabian Gulf, and the Pacific coast waters of Mexico, where *G. catenatum* and *G. impudicum* have been found alongside *Margalefidinium polykrikoides* (Margalef) F.Gómez, Richlen & D.M.Anderson, another chain-forming unarmored dinoflagellate known to cause massive fish kills (Cho et al., 2001; Cho & Costas 2004; Park & Park, 2010; Band-Schmidt et al., 2020). These three species are morphologically very similar and can be difficult to distinguish under light microscopy (Cho et al., 2001). The morphological description provided in this study represents an additional tool for differentiating between chain-forming species within the genus *Gymnodinium*. Furthermore, the co-occurrence of these species in Argentinean waters highlights the importance of considering their presence in regional monitoring programs. Given that *G. catenatum* is a toxic species, these findings have significant public health implications, particularly in areas reliant on shellfish harvesting.

ACKNOWLEDGEMENTS

We thank to the Electron Microscopy Unit, a core facility and Zeiss Reference Center at the Universidad Austral de Chile (Valdivia, Chile), for their TEM technical support. This work was partially supported by grants from the Universidad Nacional de La Plata 11/N 987, from the Consejo Nacional de Investigaciones Científicas y Técnicas PIP 1920 and from the Subsecretaría de Pesca y Acuicultura de Chile (SUBPESCA), which funds the Instituto de Fomento Pesquero (IFOP). We also thank the anonymous reviewers for their valuable comments and suggestions, which helped improve the manuscript.

BIBLIOGRAPHY

Acha, M. E.; H. Mianzan, R. A. Guerrero, J. I. Carreto, D. Giberto, N. G. Montoya & M. O. Carignan. 2008. An overview of physical and ecological processes in the Rio de la Plata Estuary. *Continental Shelf Research* 28(13): 1579-1588. DOI: https://doi.org/10.1016/j.csr.2007.01.031

Akselman, R.; J. I. Carreto & N. G. Montoya. 1998. *Gymnodinium catenatum* and autumn toxicity in northern shelf waters of Argentina. In B. Reguera, J. Blanco, M. L. Fernández & T. Wyatt (eds.), *Harmful Microalgae,* pp. 122-123. IOC-UNESCO, Paris.

Anderson, D. M., J. J. Sullivan & B. Reguera. 1989. Paralytic shellfish poisoning in Northwest Spain: The toxicity of the dinoflagellate *Gymnodinium catenatum*. *Toxicon* 27(6): 665-674. DOI: https://doi.org/10.1016/0041-0101(89)90017-2

Attaran-Fariman, G.; M. F. De Salas, A. P. Negri & C. J. S. Bolch. 2007. Morphology and phylogeny of *Gymnodinium trapeziforme* sp. nov. (Dinophyceae): A new dinoflagellate

from the southeast coast of Iran that forms microreticulate resting cysts. *Phycologia* 46(6): 644-656. DOI: https://doi.org/10.2216/07-05.1

Balech, E. 1964. El plancton de Mar del Plata durante el período 1961–1962. *Boletín del Instituto de Biología Marina* 4(1): 1-49.

Band-Schmidt, C. J.; M. G. Zumaya-Higuera, D. J. López-Cortés, I. Leyva-Valencia, S. I. Quijano-Scheggia & C. J. Hernández-Guerrero. 2020. Allelopathic effects of *Margalefidinium polykrikoides* and *Gymnodinium impudicum* in the growth of *Gymnodinium catenatum*. *Harmful Algae* 96: 101846

Bustillos-Guzmán, J. J.; C. J. Band-Schmidt, L. M. Durán-Riveroll F. E. Hernández-Sandoval, D. J. López-Cortés, E. J. Núñez-Vázquez, A. Cembella & B. Krock. 2015. Paralytic toxin profile of the marine dinoflagellate *Gymnodinium catenatum* Graham from the Mexican Pacific as revealed by LC-MS/MS. *Food Additives & Contaminants: Part A Chemistry, Analysis, Control, Exposure and Risk Assessment* 32: 381-394. DOI: https://doi.org/10.1080/19440049.2014.1000978

Cho, E. S. & E. Costas. 2004. Rapid monitoring for the potentially ichthyotoxic dinoflagellate *Cochlodinium polykrikoides* in Korean coastal waters using fluorescent probe tools. *Journal of Plankton Research* 26(2): 175-180. DOI: https://doi.org/10.1093/plankt/fbh022

Cho, E. S.; G. Y. Kim, B. D. Choi, L. L. Rhodes, T. J. Kim, G. H. Kim & J. D. Lee. 2001. A comparative study of the harmful dinoflagellates *Cochlodinium polykrikoides* and *Gyrodinium impudicum* using transmission electron microscopy, fatty acid composition, carotenoid content, DNA quantification and gene sequences. *Botanica Marina* 44: 57- 66. DOI: https://doi.org/10.1515/BOT.2001.008

Daugbjerg, N.; G. Hansen, J. Larsen & Ø. Moestrup. 2000. Phylogeny of some of the major genera of dinoflagellates based on ultrastructure and partial LSU rDNA sequence data, including the erection of three new genera of unarmoured dinoflagellates. *Phycologia* 39: 302-317. DOI: https://doi.org/10.2216/i0031-8884-39-4-302.1

Durán-Riveroll, L. M.; B. Krock, A. Cembella, J. Peralta-Cruz, J. J. Bustillos-Guzmán & C. J. Band-Schmidt. 2017. Characterization of benzoyl saxitoxin analogs from the toxigenic marine dinoflagellate *Gymnodinium catenatum* by hydrophilic interaction liquid ion-chromatography-tandem mass spectrometry. *Natural Products Chemistry & Research* 5(4). DOI: https://doi.org/10.4172/2329-6836.1000275

Edvardsen, B.; K. Shalchian-Tabrizi, K. S. Jakobsen, L. K. Medlin, E. Dahl, S. Brubak & E. Paasche. 2003. Genetic variability and molecular phylogeny of *Dinophysis* species (Dinophyceae) from Norwegian waters inferred from single cell analyses of rDNA. *Journal of Phycology* 39: 395-408. DOI: https://doi.org/10.1046/j.1529-8817.2003.01252.x

Estrada, M.; F. J. Sánchez & S. Fraga. 1984. *Gymnodinium catenatum* (Graham) en las rías gallegas (NO de España). *Investigación Pesquera* 48: 31-40.

Fraga, S.; I. Bravo, M. Delgado, J. M. Franco & M. Zapata. 1995. *Gyrodinium impudicum* sp. nov. (Dinophyceae), a non-toxic, chain-forming, red tide dinoflagellate. *Phycologia* 34: 514-521. DOI: https://doi.org/10.2216/i0031-8884-34-6-514.1

Framiñan, M. B. & O. B. Brown. 1996. Study of the Rio de la Plata turbidity front. Part I: Spatial and temporal distribution. *Continental Shelf Research* 16: 1259-1282. DOI: https://doi.org/10.1016/0278-4343(95)00071-2

Gómez, N.; P. R. Hualde, M. Licursi & D. E. Bauer. 2004. Spring phytoplankton of Río de la Plata: A temperate estuary of South America. *Estuarine, Coastal and Shelf Science* 61: 301-309. DOI: https://doi.org/10.1016/j.ecss.2004.05.007

Graham, H. 1943. *Gymnodinium catenatum*, a new dinoflagellate from the Gulf of California. *Transactions of the American Microscopical Society* 62: 259-261. DOI: https://doi.org/10.2307/3223028

Gu, H.; Z. Luo, K. N. Mertens, A. M. Price, R. E. Turner & N. N. Rabalais. 2015. Cyst-motile stage relationship, morphology, ultrastructure, and molecular phylogeny of the Gymnodinioid Dinoflagellate *Barrufeta resplendens* comb. nov., formerly known as *Gyrodinium resplendens*, isolated from the Gulf of Mexico. *Journal of Phycology* 51: 990-999. DOI: https://doi.org/10.1111/jpy.12342

Hallegraeff, G. M.; S. I. Blackburn, M. A. Doblin & C. J. S. Bolch. 2012. Global toxicology, ecophysiology and population relationships of the chain forming PST dinoflagellate *Gymnodinium catenatum*. *Harmful Algae* 14: 130-143. DOI: https://doi.org/10.1016/j.hal.2011.10018

Huelsenbeck, J. P. & F. Ronquist. 2001. MRBAYES: Bayesian inference of phylogenetic trees. *Bioinformatics, 17,* 754-755. DOI: https://doi.org/10.1093/bioinformatics/17.8.754

Kumar, S.; G. Stecher, M. Li, C. Knyaz & K. Tamura. 2018. MEGA X: Molecular evolutionary genetics analysis across computing platforms. *Molecular Biology and Evolution* 35: 1547-1549. DOI: https://doi.org/10.1093/molbev/msy096

Larkin, M. A.; G. Blackshields, N. P. Brown, R. Chenna, P. A. McGettigan, H. McWilliam, F. Valentin, I. M. Wallace, A. Wilm, R. Lopez, J. D. Thompson, T. J. Gibson & D. G. Higgins. 2007. Clustal W and Clustal X version 2.0. *Bioinformatics* 23: 2947-2948. DOI: https://doi.org/10.1093/bioinformatics/btm404

Lassus, P.; N. Chomérat, P. Hess & E. Nézan. 2016. Toxic and harmful microalgae of the world ocean/Micro-algues

toxiques et nuisibles de l'océan mondial. *IOC Manuals and Guides* 68*:* 1-523.

Liu, M.; H. Gu, B. Krock, Z. Luo & Y. Zhang. 2020. Toxic dinoflagellate booms of *Gymnodinium catenatum* and their cysts in Taiwan Strait and their relationship to global populations. *Harmful Algae* 97: 101868. DOI: https://doi.org/10.1016/0041-0101(87)90267-4

Luo, Z.; Z. Hu, Y. Tang, K. N. Mertens, C. P. Leaw, P. T. Lim, S. T. Teng, L. Wang & H. Gu. 2018. Morphology, ultrastructure, and molecular phylogeny of *Wangodinium sinense* gen. et sp. nov. (Gymnodiniales, Dinophyceae) and revisiting of *Gymnodinium dorsalisulcum* and *Gymnodinium impudicum*. *Journal of Phycology* 54: 744-761. DOI: https://doi.org/10.1111/jpy.12780

Mee, L. D.; M. Espinosa & G. Diaz. 1986. Paralytic shellfish poisoning with a *Gymnodinium catenatum* red tide on the Pacific coast of Mexico. *Marine Environmental Research* 19: 77-92. DOI: https://doi.org/10.1016/0141-1136(86)90040-1

Montoya, N. G.; R. Akselman, M. O. Carignan & J. I. Carreto. 2006. Pigment profile and toxin composition during a red tide of *Gymnodinium catenatum* Graham and *Myrionecta rubra* (Lohman) Jankowski in coastal waters off Mar del Plata, Argentina. *African Journal of Marine Science* 28: 199-202. DOI: https://doi.org/10.2989/18142320609504147

Negri, A. P.; C. J. S. Bolch, S. Geier, D. H. Green, T.-G. Park & S. I. Blackburn. 2007. Widespread presence of hydrophobic paralytic shellfish toxins in *Gymnodinium catenatum*. *Harmful Algae* 6: 774-780. DOI: https://doi.org/10.1016/j.hal.2007.04.001

Nei, M. & S. Kumar. 2000. *Molecular Evolution and Phylogenetics*. Oxford University Press, New York, 333 pp.

Oshima, Y.; M. Hasegawa, T. Yasumoto, G. M. Hallegraeff & S. Blackburn. 1987. Dinoflagellate *Gymnodinium catenatum* as the source of paralytic shellfish toxins in Tasmanian shellfish. *Toxicon* 25: 1105-1111. DOI: https://doi.org/10.1016/0041-0101(87)90267-4

Oshima, Y.; S. I. Blackburn & G. M. Hallegraeff. 1993. Comparative study on paralytic shellfish toxin profiles of the dinoflagellate *Gymnodinium catenatum* from three different countries. *Marine Biology* 116: 471-476. DOI: https://doi.org/10.1007/BF00350064

Park, T. -G. & Y. -T. Park. 2010. Detection of *Cochlodinium polykrikoides* and *Gymnodinium impudicum* (Dinophyceae) in sediment samples from Korea using real-time PCR. *Harmful Algae* 9: 59-65.

Rees, A. J. J. & G. M. Hallegraeff. 1991. Ultrastructure of the toxic, chain-forming dinoflagellate *Gymnodinium catenatum* (Dinophyceae). *Phycologia* 30: 90-105. DOI: https://doi.org/10.2216/i0031-8884-30-1-90.1

Reñé, A.; C. T. Satta, E. Garcés, R. Massana, M. Zapata, S. Anglès & J. Camp. 2011. *Gymnodinium litoralis* sp. nov. (Dinophyceae), a newly identified bloom-forming dinoflagellate from the NW Mediterranean Sea. *Harmful Algae* 12: 11-25. DOI: https://doi.org/10.1016/j.hal.2011.08.008

Rodríguez, I.; A. Alfonso, J. M. Gonzalez-Jartin, M. R. Vieytes & L.-M. Botana. 2018. A single run UPLC-MS/MS method for detection of all EU-regulated marine toxins. *Talanta* 189: 622-628. DOI: https://doi.org/10.1016/j.talanta.2018.07.050

Scholin, C. A.; M. Herzog, M. Sogin & D. M. Anderson. 1994. Identification of group- and strain-specific genetic markers for globally distributed *Alexandrium* (Dinophyceae). II. Sequence analysis of a fragment of the LSU rRNA gene. *Journal of Phycology* 30: 999-1011. DOI: https://doi.org/10.1111/j.0022-3646.1994.00999.x

Sunesen, I.; A. S. Lavigne, A. Goya & E. A. Sar. 2014. Episodios de toxicidad en moluscos de aguas marinas costeras de la Provincia de Buenos Aires (Argentina) asociados a algas toxígenas (marzo de 2008-marzo de 2013). *Boletín de la Sociedad Argentina de Botánica* 49: 327-339.

Sunesen, I.; F. Rodríguez Hernández, D. Aguiar Juárez, J. A. Tardivo Kubis, A. S. Lavigne, A. Rossignoli; P. Riobó & E. A. Sar. 2020. Morphology, genetics and toxin profile of *Prorocentrum texanum* (Dinophyceae) from Argentinian marine coastal waters. *Phycologia* 59: 634-650. DOI: https://doi.org/10.1080/00318884.2020.1830552

Tamura, K. & M. Nei. 1993. Estimation of the number of nucleotide substitutions in the control region of mitochondrial DNA in humans and chimpanzees. *Molecular Biology and Evolution* 10: 512-526. DOI: https://doi.org/10.1093/oxfordjournals.molbev.a040023

Taylor, F. J. R.; Y. Fukuyo, J. Larsen & G. M. Hallegraeff. 2004. Taxonomy of harmful dinoflagellates. In G. M. Hallegraeff, D. M. Anderson & A. D. Cembella (eds.), *Manual on harmful marine Microalgae,* pp. 389-432. IOC Manuals and Guides 33. IOC-UNESCO, Paris.

Utermöhl, H. 1958. Zur Vervollkommnung der quantitativen Phytoplankton-Methodik: Mit 1 Tabelle und 15 Abbildungen im Text und auf 1 Tafel. *SIL Communications, 1953–1996, Mitteilungen Internationale Vereinigung für Theoretische und Angewandte Limnologie* 9: 1-38. DOI: https://doi.org/10.1080/05384680.1958.11904091

SUPPLEMENTARY INFORMATION

Table S1. List of species, sampling locations, strains codes, Genbank accession number and references used in LSU rDNA phylogeny.

Species	Sampling location	Strain	Accession number	References
Barrufeta bravensis	Mediterranean coast of Catalonia, Spain	VGO863	FN647672	Sampedro *et al.* (2011)
Barrufeta bravensis	Mediterranean coast of Catalonia, Spain	VGO864	FN647673	Sampedro *et al.* (2011)
Barrufeta bravensis	Mediterranean coast of Catalonia, Spain	VGO859	FN647674	Sampedro *et al.* (2011)
Barrufeta bravensis	Mediterranean coast of Catalonia, Spain	VGO862	FN647675	Sampedro *et al.* (2011)
Barrufeta resplendens	Gulf of Mexico, USA	GM16	KT203381	Gu *et al.* (2015)
Barrufeta resplendens	Gulf of Mexico, USA	GM17	KT203382	Gu *et al.* (2015)
Gymnodinium catenatum	**Samborombón Bay, Argentina**	**LPCc043**	**OP850345**	**This study**
Gymnodinium catenatum	Vigo, Spain	Nd	AF200672	Hansen *et al.* (2000)
Gymnodinium catenatum	Western Singapore Port, Singapore	GCSG2	AY036121	Holmes *et al.* (2002)
Gymnodinium catenatum	Deep Bay, Hong Kong, P.R. China	GCHK53	AY036123	Holmes *et al.* (2002)
Gymnodinium catenatum	Punte del Este, Uruguay	GCUR43	AY036124	Holmes *et al.* (2002)
Gymnodinium catenatum	Chindong, South Korea	GCCW991	AY036125	Holmes *et al.* (2002)
Gymnodinium catenatum	Deukyrang Bay, South Korea	DC99A44	AY036127	Holmes *et al.* (2002)
Gymnodinium catenatum	Kaitaia Spat, North Island, New Zealand	CAWD101	AY036128	Holmes *et al.* (2002)
Gymnodinium catenatum	Cowans Creek, New South Wales, Australia	GCCC21	AY036072	Holmes *et al.* (2002)
Gymnodinium catenatum	Yellow Sea, China	GCDL01	KF234065	Luo *et al.* (2018)
Gymnodinium catenatum	Yellow Sea, China	GCQD01	KF234066	Luo *et al.* (2018)
Gymnodinium catenatum	Ría deVigo, Spain	CCMP414	DQ779990	Unpublished
Gymnodinium catenatum	Ría deVigo, Spain	GC19V	AF375856	Unpublished
Gymnodinium catenatum	coast of Cadiz, Strait of Gibraltar, Spain	GC36AM	AF375857	Unpublished
Gymnodinium catenatum	Ria de Vigo, Galicia	GC12V	AF375855	Unpublished
Gymnodinium fuscum	Denmark	CCMP1677	AF200676	Daugbjerg *et al.* (2000); Reñé *et al.* (2011)
Gymnodinium dorsalisulcum	Australia	SM28	DQ336190	Kang *et al.* (2013)
Gymnodinium dorsalisulcum	Australia	KDAAD	DQ837533	Kang *et al.* (2013)
Gymnodinium dorsalisulcum	Sanya, South China Sea, China	TIO09	MH732682	Luo *et al.* (2018)
Gymnodinium dorsalisulcum	Malaysia	SS10H1	MH732684	Luo *et al.* (2018)
Gymnodinium impudicum	**Samborombón Bay, Argentina**	**LPCc044**	**OP851763**	**This study**
Gymnodinium impudicum	Korea	GrIp02	DQ779993	Ki & Han (2007)
Gymnodinium impudicum	Gulf of Naples, Italy	JL30	AF200674	Reñé *et al.* (2011)
Gymnodinium impudicum	Valencia, Spain	Gy2VA	JN400079	Reñé *et al.* (2011)
Gymnodinium impudicum	Concarneau Bay, France	IFR1020	KJ508393	Nézan *et al.* (2014)
Gymnodinium impudicum	Catalan coast, Spain	ICMB204	KP790184	Reñé *et al.* (2015)
Gymnodinium impudicum	China	TIO335	MH732685	Luo *et al.* (2018)
Gymnodinium impudicum	Corsica, Mediterranean Sea, France	TIO251	MH732686	Luo *et al.* (2018)
Gymnodinium impudicum	Bahía Concepción, Mexico	GIBACO-1	MT070782	Band-Schmidt *et al.* (2020)
Gymnodinium litoralis	Catalonia, Spain	ICMB224	JN400080	Reñé *et al.* (2011)

Gymnodinium litoralis	Sardinia, Italy	UNISS1	JN400084	Reñé *et al.* (2011)
Gymnodinium microreticulatum	Uruguay	GMUR02	AY916539	Patil *et al.* (2005)
Gymnodinium microreticulatum	Australia	GMNC01	AY036078	Sampedro *et al.* (2011)
Gymnodinium nolleri	Denmark	DK4	AF200673	Ellegaard & Oshima (1998)
Gymnodinium nolleri	Spain	VGO663	FN649408	Sampedro *et al.* (2011)
Gymnodinium nolleri	Spain	VGO922	FN649409	Sampedro *et al.* (2011)
Gymnodinium plasticum	Plastic Lake, Canada	TIO826	KY688184	Wang *et al.* (2017)
Gymnodinium smaydae	Shiwha Bay, Korea	GSSW10	HG005135	Kang *et al.* (2013)
Gymnodinium trapeziforme	Pasabander, South coast of Iran	GYPC02	EF192414	Attaran-Fariman *et al.* (2007); Kang *et al.* (2013)
Lepidodinium chlorophorum	Sylt, Germany	K-0539	AF200669	Hansen *et al.* (2000)
Lepidodinium chlorophorum	Brest Bay, France	IFR-LCH-01L	KJ508396	Nézan *et al.* (2014)
Lepidodinium viride	South Africa	Nd	DQ499645	Unpublished
Lepidodinium viride	False Bay, South Africa	NA	AY464689	Unpublished
Wangodinium sinense	Lianyungang, China	GLY03	MH732679	Luo *et al.* (2018)
Wangodinium sinense	Xiamen Harbor, China	G27	MH732680	Luo *et al.* (2018)
Wangodinium sinense	Beihai, China	GBH03	MH732681	Luo *et al.* (2018)
Wangodinium sinense	Busan, South Korea	WsLomme01	OL699923	Unpublished

REFERENCES

Attaran-Fariman, G.; M. F. De Salas, A. P. Negri & C. J. S. Bolch. 2007. Morphology and phylogeny of *Gymnodinium trapeziforme* sp. nov. (Dinophyceae): A new dinoflagellate from the southeast coast of Iran that forms microreticulate resting cysts. *Phycologia* 46(6): 644-656. DOI: https://doi.org/10.2216/07-05.1

Band-Schmidt, C. J.; M. G. Zumaya-Kiguera, D. J. López-Cortés, I. Leyva-Valencia, S. I. Quijano-Scheggia & C. J. Hernández-Guerrero. 2020. Allelopathic effects of *Margalefidinium polykrikoides* and *Gymnodinium impudicum* in the growth of *Gymnodinium catenatum*. *Harmful Algae* 96: 101846. DOI: https://doi.org/10.1016/j.hal.2020.101846

Ellegaard, M. & Y. Oshima. 1998. *Gymnodinium nolleri* Ellegaard et Moestrup sp. ined. (Dinophyceae) from Danish waters, a new species producing *Gymnodinium catenatum*-like cysts: molecular and toxicological comparisons with Australian and Spanish strains of *Gymnodinium catenatum*. *Phycologia* 37: 369-378. DOI: https://doi.org/10.2216/i0031-8884-37-5-369.1

Hansen, G.; N. Daugbjerg & P. Henriksen. 2000. Comparative study of *Gymnodinium mikimotoi* and *Gymnodinium aureolum*, comb. nov. (=*Gyrodinium aureolum*) based on morphology, pigment composition, and molecular data. *Journal of Phycology* 36: 394-410. DOI: https://doi.org/10.1046/j.1529-8817.2000.99172.x

Holmes, M. J.; C. J. S. Bolch, D. H. Green, A. D. Cembella & S. L. Ming Teo. 2002. Singapore isolates of the Dinoflagellate *Gymnodinium catenatum* (Dinophyceae) produce a unique profile of Paralytic Shellfish Poisoning Toxins. *Journal of Phycology* 39: 96-106. DOI: https://doi.org/10.1046/j.1529-8817.2002.01153.x

Kang, N. S.; H. J. Jeong, Ø. Moestrup, S. Y. Lee, A. Lim; Suk, T. Y. Jang, K. H. Lee, M. J. Lee, S. H. Jang, E. Potvin, S. K. Lee & J. H. Noh. 2013. *Gymnodinium smaydae* n. sp., a new planktonic phototrophic dinoflagellate from the coastal waters of Western Korea: morphology and molecular characterization. *Journal of Eukaryotic Microbiology* 61: 182-203. DOI: https://doi.org/10.1111/jeu.12098

Ki, J.-S. & M.-S. Han. 2007. Cryptic long internal repeat sequences in the ribosomal DNA ITS1 gene of the dinoflagellate *Cochlodinium polykrikoides* (Dinophyceae): a 101 nucleotide six-repeat track with a palindrome-like structure. *Genes & Genetic Systems* 82: 161-166. DOI: https://doi.org/10.1266/ggs.82.161

Luo, Z.; Z. Hu, Y. Tang, K. N. Mertens, C. P. Leaw, P. T. Lim, S. T. Teng, L. Wang & H. Gu. 2018. Morphology, ultrastructure, and molecular phylogeny of *Wangodinium sinense* gen. et sp. nov. (Gymnodiniales, Dinophyceae) and revisiting of *Gymnodinium dorsalisulcum* and *Gymnodinium*

impudicum. *Journal of Phycology* 54: 744-761. DOI: https://doi.org/10.1111/jpy.12780

Nézan, E.; R. Siano, S. Boulben, C. Six, G. Bilien, K. Chèze, A. Duval, S. Le Panse, J. Quéré & N. Chomérat. 2014. Genetic diversity of the harmful family Kareniaceae (Gymnodiniales, Dinophyceae) in France, with the description of *Karlodinium gentienii* sp. nov.: a new potentially toxic dinoflagellate. *Harmful Algae* 40: 75-91. DOI: https://doi.org/10.1016/j.hal.2014.10.006

Patil, J. G.; R. M. Gunasekera, B. E. Deagle, N. J. Bax & S. I. Blackburn. 2005. Development and evaluation of a PCR based assay for detection of the toxic dinoflagellate, *Gymnodinium catenatum* (Graham) in ballast water and environmental samples. *Biological Invasions* 7: 983-994. DOI: https://doi.org/10.1007/s10530-004-3119-8

Reñé, A.; C. T. Satta, E. Garcés, R. Massana, M. Zapata, S. Anglès & J. Camp. 2011. *Gymnodinium litoralis* sp. nov. (Dinophyceae), a newly identified bloom-forming dinoflagellate from the NW Mediterranean Sea. *Harmful Algae* 12: 11-25. DOI: https://doi.org/10.1016/j.hal.2011.08.008

Sampedro, N.; S. Fraga, A. Penna, S. Casabianca, M. Zapata, C. Fuentes Grünewald, P. Riobó & J. Camp. 2011. *Barrufeta bravensis* gen. nov. sp. nov. (Dinophyceae); a new bloom-forming species from the Northwest Mediterranean Sea. *Journal of Phycology* 47: 375-392. DOI: https://doi.org/10.1111/j.1529-8817.2011.00968.x

Wang, N.; Z. Luo, K. N. Mertens, F. M. G. McCarthy, L. Gu & H. Gu. 2017. Cyst-motile stage relationship and molecular phylogeny of a new freshwater dinoflagellate *Gymnodinium plasticum* from Plastic Lake, Canada. *Phycological Research* 65: 312-321. DOI: https://doi.org/10.1111/pre.12190

Table S2. MS/MS conditions used for the MRM acquisition of data for the PSTs analyzed. CAV: cell accelerator voltage; ESI: electrospray ionization; m/z: mass to charge ratio; m sec: milliseconds; Pos: positive; V: voltage.

Analog	CAV	ESI Mode	Precursor ion (m/z)	Product ion (m/z)	Dwell (m sec)	Fragmentor (V)	Collision E (V)
STX	2	Pos	300	204	15	108	24
STX	2	Pos	300	60.2	15	108	40
NEO	2	Pos	316	298.1	15	112	20
NEO	2	Pos	316	110.1	15	112	52
GTX1	2	Neg	410.1	367.1	15	110	16
GTX1	2	Neg	410.1	349.1	15	110	20
GTX4	4	Pos	412.1	332.1	15	80	12
GTX4	4	Pos	412.1	314.1	15	80	17
GTX2	2	Neg	394.1	351.1	15	151	12
GTX2	2	Neg	394.1	333.1	15	151	20
GTX3	2	Pos	396.1	110.1	15	108	56
GTX3	2	Pos	396.1	298.1	15	108	16
C1	4	Neg	474	351	15	110	29
C1	4	Neg	474	121.9	15	110	37
C2	4	Pos	396.1	298.1	15	110	21
C2	4	Neg	474	121.9	15	110	37
B1	2	Pos	380.1	300.1	15	132	24
B1	2	Neg	378.1	360	15	147	12
B1	2	Neg	378.1	122	15	147	24
B2	4	Pos	396	316	15	68	8
B2	1	Neg	394.2	121.9	15	129	21
dcSTX	2	Pos	257	126	15	128	20
dcSTX	2	Pos	257	84.1	15	128	32
dcNEO	2	Pos	273.1	225.1	50	130	5

dcNEO	2	Pos	273.1	126.1	50	130	18
dcGTX2	2	Neg	351.1	333.1	15	156	16
dcGTX2	2	Neg	351.1	164	15	156	32
dcGTX3	2	Pos	353.1	335.1	15	89	2
dcGTX3	2	Pos	353.1	255.1	15	89	17
GC1	4	Pos	473	455	15	110	10
GC1	4	Pos	473	393	15	110	15
GC1	4	Pos	473	375	15	110	15
GC2	4	Pos	473	455	15	110	10
GC2	4	Pos	473	393	15	110	15
GC2	4	Pos	473	375	15	110	15
GC3	4	Pos	377	359	15	110	12
GC3	4	Pos	377	257	15	110	20
GC4	4	Pos	489	471	15	110	10
GC4	4	Pos	489	409	15	110	15
GC4	4	Pos	489	391	15	110	20
GC5	4	Pos	489	471	15	110	10
GC5	4	Pos	489	409	15	110	15
GC5	4	Pos	489	391	15	110	20
GC6	4	Pos	393	375	15	110	12
GC6	4	Pos	393	273	15	110	20
GC1a	4	Pos	489	471	15	110	10
GC1a	4	Pos	489	409	15	110	20
GC2a	4	Pos	489	471	15	110	10
GC2a	4	Pos	489	409	15	110	20
GC3a	4	Pos	393	375	15	110	10
GC3a	4	Pos	393	257	15	110	20
GC4a	4	Pos	504	487	15	110	10
GC4a	4	Pos	504	425	15	110	15
GC5a	4	Pos	504	487	15	110	10
GC5a	4	Pos	504	425	15	110	15
GC6a	4	Pos	409	391	15	110	10
GC6a	4	Pos	409	273	15	110	15
GC1b	4	Pos	553	393	15	110	15
GC2b	4	Pos	553	393	15	110	15
GC3b	4	Pos	457	377	15	110	15
GC4b	4	Pos	569	409	15	110	15
GC5b	4	Pos	569	409	15	110	15
GC6b	4	Pos	473	393	15	110	15